ChemComm

Accepted Manuscript

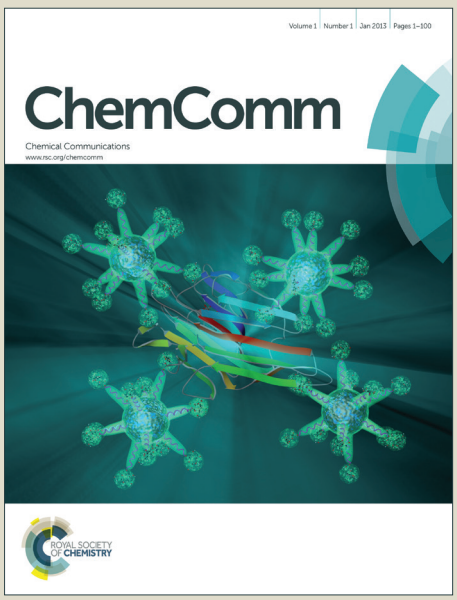

This is an *Accepted Manuscript*, which has been through the Royal Society of Chemistry peer review process and has been accepted for publication.

Accepted Manuscripts are published online shortly after acceptance, before technical editing, formatting and proof reading. Using this free service, authors can make their results available to the community, in citable form, before we publish the edited article. We will replace this *Accepted Manuscript* with the edited and formatted *Advance Article* as soon as it is available.

You can find more information about *Accepted Manuscripts* in the Information for Authors.

Please note that technical editing may introduce minor changes to the text and/or graphics, which may alter content. The journal's standard Terms & Conditions and the Ethical guidelines still apply. In no event shall the Royal Society of Chemistry be held responsible for any errors or omissions in this *Accepted Manuscript* or any consequences arising from the use of any information it contains.

ROYAL SOCIETY OF CHEMISTRY

www.rsc.org/chemcomm

Chemical communications RSCPublishing

COMMUNICATION

Non-covalent double functionalization of carbon nanotubes with a NADH oxidation Ru(II)-based molecular catalyst and a NAD-dependent glucose dehydrogenase

Cite this: DOI: 10.1039/xoxxoooooox

Received ooth January 2012,
Accepted ooth January 2012

DOI: 10.1039/xoxxoooooox

www.rsc.org/

B. Reuillard,[a] A. Le Goff,[a*] and S. Cosnier[a*]

We report the double functionalization of multiwalled carbon nanotube electrodes by two functional pyrene molecules. In combination, immobilized Ru(II)-based NADH oxidation catalyst and glucose dehydrogenase achieves highly efficient glucose oxidation with low overpotential of -0.10 V and high current densities of 6 mA cm^{-2}.

NAD-dependent dehydrogenases are versatile enzymes, having the great advantage of oxidizing a wide range of relevant substrates such as glucose, lactate, or alcohols. These enzymes were thus intensively investigated in applications ranging from biosensing to biosynthesis or biofuel cells. In particular, dehydrogenase-based biofuel cells are envisioned for harvesting energy from oxidation of glucose[1], alcohols[2] or L-lactate[3]. Furthermore, their wide biodiversity makes these enzymes also promising for enzyme cascade system in which a biofuel can be fully oxidized by successive multi-enzymatic oxidation performed by immobilized dehydrogenases, using NADH/NAD as ubiquitous cofactor.[2]However, such process requires, an efficient electrochemical catalyst for the NADH oxidation in order to maximize anodic catalytic currents and minimize the NADH oxidation overpotential. Although the redox potential of NADH is -0.56V vs SCE, its oxidation often requires high overpotentials. In this context, organic dyes and metal complexes have demonstrated low overpotential oxidation for NADH[4–6]. In particular, we have recently demonstrated that a Ru(II) complex, previously developed by H. Abruna et al [7] for low-potential oxidation of NADH, could be combined to carbon nanotubes for efficient oxidation of NADH, via the electrogeneration of a metallopolymer at the surface of carbon nanotubes (CNTs) sidewalls.[8] CNTs are widely investigated as an electrode material for both electrocatalytic and bioelectrocatalytic applications. Their ability to immobilize high concentration of redox catalysts and to efficiently transfer electrons have made this nanomaterial a key material in designing electrodes for molecular electrocatalysis[9,10]. In addition, CNTs can be functionalized by a large variety of covalent or non-covalent techniques. We and others have especially developed the non-covalent functionalization of CNTs for immobilization of molecular electrocatalysts based on modified transition-metal complexes[11–13]. Non-covalent functionalization is based on the strong pi-pi interactions between pyrene and CNT sidewalls. By similar means, we and other have also developed the immobilization of redox enzymes by pyrene derivatives previously pi-stackedon CNTs[14–17]. In addition, it was recently demonstrated that covalent or non-covalent multiple functionalization of carbon nanotube sidewalls could have promising applications in drug delivery[18,19] and biosensing[20] applications. Here we report the first example of a double functionalization of Multi-Walled CNTs (MWCNTs) with a molecular catalyst and an enzyme for a combined electroenzymatic process. Namely, a glucose dehydrogenase (GDH) was chemically grafted on MWCNTS via a N-hydrosuccinimide-modified pyrene to assume the enzymatic oxidation of glucose in presence of NAD^+. In addition, an original Ru(II) complex, bearing phenanthrolinequinone (phendione) and pyrene-modified bipyridine ligands was used for the electrocatalytic oxidation of NADH cofactor. With the aim to design new glucose biofuel cells, these bi-functionalized MWCNT electrodes were electrochemically characterized and investigated for the improved glucose oxidation .

An original [(1,10-phenathroline-5,6-dione)$_2$((4,4'-bis(4-pyrenyl-1-ylbutyloxy)-2,2'-bipyridine)Ru(II)] hexafluoro-phosphate complex (**RuQ-pyrene)** was synthesized by refluxing [Ru(1,10-phenanthroline-5,6-dione)$_2$Cl$_2$] with 4,4'-bis(4-pyrenyl-1-ylbutyloxy)-2,2'-bipyridine) in ethylene glycol. **RuQ-pyrene** was fully characterized by ^{1}H NMR, mass spectroscopy and UV-visible spectrophotometry. Its redox behaviour was characterized using cyclic voltammetry in 0.1M

ChemComm Accepted Manuscript

TBAP/MeCN (figure 1). The complex exhibits one reversible peak system at $E_{1/2}^{ox}$= 0.98V corresponding to the $Ru^{III/II}$ reversible redox system and an overlapping irreversible oxidation peak around E_p^{ox} = 1 V corresponding to the oxidation of the two pyrene groups. Two quasi-reversible peak systems at $E_{1/2}(Q^{-}/Q)$ = -0.50V and $E_{1/2}(Q^{2-}/Q^{-})$ = -1.30V were attributed to the two successive one-electron reduction of the phendione ligand. The one-electron reduction of the bipyridine ligand (bpy^{-}/bpy) leads to a reversible couple at -2.34V.

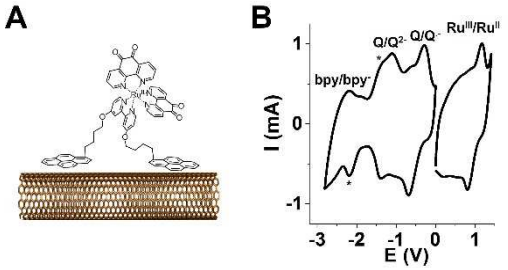

Figure 1. (A) Schematic representation of the preparation of MWCNT/**RuQ-pyrene**electrode. (B) Electrochemical characterisation of a **RuQ-pyrene**-functionalized MWCNT electrode by cyclic voltammetry in MeCN + 0.1M TBAP (v= 100 mV s^{-1}, starred peaks corresponds to charge trapping)

The establishment of pi-pi stacking interactions between pyrene moieties of the Ru complex and graphene planes of the MWCNT film affords its physisorption on MWCNT electrodes. A MWCNT electrode was simply incubated for 60 min in 0 to 8 mM **RuQ-pyrene** solution. After several washings, the modified MWCNT electrode was characterized by cyclic voltammetry in pure electrolyte. In MeCN, the **RuQ-pyrene**-functionalized MWCNT electrode displays the characteristic redox activity of immobilized **RuQ-pyrene**, accompanied with irreversible charge trapping peaks (starred peaks at -1.4 and -2.2V), often observed for immobilized redox species (figure 1B)[21]. In water, a reversible bielectronic peak system is observed at -0.02 V, corresponding to the electroactivity of the phendione redox couple QH_2/Q in water. Oxidation and reduction peak currents are highly stable upon scanning and are directly proportional to the scan rate. As expected, this electrochemical behaviour reflects the characteristics of firmly immobilized redox specie. Surface concentrations were estimated by integration of the charge under the anodic peak current. Figure 2A displays the variation of the surface coverage measured in water over the initial incubating **RuQ-pyrene** solution in DMF at 25°C.

The **RuQ-pyrene** surface coverage increases with the starting concentration in solution, following a simple Langmuir isotherm, according to equation 1.

$$\Gamma_{eq,Ru} = \frac{\Gamma_{max} \times K_{Ru} \times [\boldsymbol{RuQ-pyrene}]}{1 + K_{Ru} \times [\boldsymbol{RuQ-pyrene}]} \quad (1)$$

where $\Gamma_{eq,Ru}$ is the equilibrium surface coverage of **RuQ-pyrene**, Γ_{max} is the saturating surface coverage and K_{Ru} is the association constant of **RuQ-pyrene** with MWCNTs in DMF at 25°C. The best fit was achieved with a Γ_{max} of 17.8 nmol cm^{-2} and K_{Ru} of 1900 L mol^{-1}. It is noteworthy that we did not observe any influence of the incubation time on the **RuQ-pyrene** surface coverage between one and 60 minutes, showing that the equilibrium of the pi-pi interactions is rapidly reached.

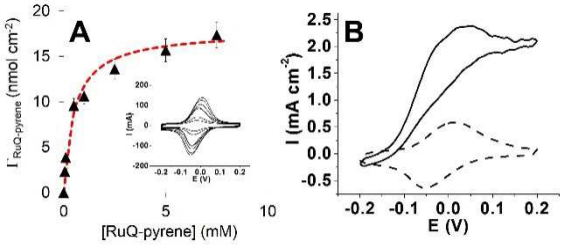

Figure 2. (A) Variation of the **RuQ-pyrene** surface coverage with incubating **RuQ-pyrene** concentrations in DMF accompanied with the fitting binding isotherm (red dashed line); (inset) : Cyclic voltammetry of **RuQ-pyrene**-functionalized MWCNT electrodes performed in 0.2 M PBS, after incubation in different concentrations of Ru complex in DMF (v= 10 mV s^{-1}) ; (B) Cyclic voltammograms of MWCNT/ **RuQ-pyrene** electrode ($\Gamma_{RuQ\text{-}pyrene}$ = 15 nmol cm^{-2}) in absence (dashed line) and presence (full line) of NADH (10mM) in PBS (0.2 M, pH 7) at RT (v = 10 mV s-1).

The maximum surface coverage is equivalent to 220 layers of closely-packed **RuQ-pyrene,** underlining the high specific surface of MWCNT films. This is confirmed by scanning electron microscopy (SEM) image of the surface of the **RuQ-pyrene**-functionalized MWCNT electrode (figure S1).

Electrocatalytic properties of these functionalized electrodes were studied in water. We investigated the redox behaviour of phendione ligand in the presence of NADH (figure 2B). In the presence of 10 mM NADH, an irreversible anodic peak current is observed, starting at -0.10 V, at the foot of the QH_2/Q oxidation peak, confirming the electrocatalytic properties of **RuQ-pyrene**-functionalized MWCNTs. Maximum catalytic current of 2.5 mA cm^{-2} was achieved at 10 mM NADH.

Thanks to the easy self-assembly of pyrene molecules onto MWCNT sidewalls, we studied the double functionalization of MWCNT electrodes with both **RuQ**-pyrene and **NHS-pyrene (figure 3A)**.

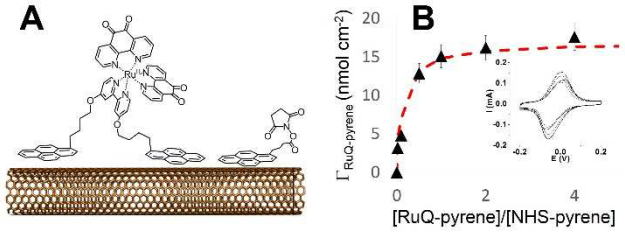

Figure 3. (A) Schematic representation of the double functionalization of MWCNTs with **RuQ-pyrene** and **NHS-pyrene**; (B) Variation of the **RuQ-pyrene** surface coverage with incubating **RuQ-pyrene/NHS-pyrene** concentration ratiosin DMF accompanied with the fitting binding isotherm (red dashed line); (inset) : Cyclic voltammetry of **RuQ-pyrene**-functionalized MWCNT electrodes performed in 0.2 M PBS (v = 10 mV s-1), using different incubating concentrations of **RuQ-pyrene** and **NHS-pyrene** in DMF

MWCNT electrodes were simply incubated in solution containing different ratios of **RuQ-pyrene** and 1-pyrenebutyric acid N-hydroxysuccinimide ester (**NHS-pyrene)**. As investigated for **RuQ-pyrene** incubating solutions, we measured the **RuQ-pyrene** surface coverage by electrochemistry in water.

ChemComm Accepted Manuscript

This journal is © The Royal Society of Chemistry 2012

In this case, the **RuQ-pyrene** surface coverage increases with increasing **RuQ-pyrene/NHS-pyrene** concentration ratios. The evolution of the **RuQ-pyrene** surface coverage follows a binary competitive Langmuir isotherm, according to equation 2:

$$\Gamma_{eq,Ru} = \frac{\Gamma_{max} \times K_{Ru} \times [\boldsymbol{RuQ-pyrene}]}{1 + K_{Ru} \times [\boldsymbol{RuQ-pyrene}] + K_{NHS} \times [\boldsymbol{NHS-pyrene}]} \quad (2)$$

where K_{NHS} is the association constant of **NHS-pyrene** with MWCNTs in DMF at 25°C. This equation can be applied because**NHS-pyrene** and **RuQ-pyrene** do not interact in solution in the range of 0 to 10 mM and interact with same adsorption sites on CNT sidewalls. This model is corroborated by the fact that neither K_{Ru} (1900 L mol^{-1}) nor Γ_{max} (17.8 nmol cm^{-2}) are influenced by the presence of **NHS-pyrene**. Furthermore, a K_{NHS} of 180 L mol^{-1} was determined, which is more than ten times lower than K_{Ru}. This implies that **RuQ-pyrene** interactsstronger than**NHS-pyrene** with MWCNT sidewalls. This phenomenon likely arises from the presence of two pyrene groups in **RuQ-pyrene** that facilitate its adsorption and reinforce the mechanical stability of the immobilized form.

Finally, these electrodes were incubated in a 2mg mL^{-1} solution of GDH (figure 4). Figure 4B shows a typical CV in the presence of 160mM glucose and 10mM of NAD^+. The addition of glucose triggers the appearance of an irreversible catalytic wave, starting at -0.10V and corresponding to the oxidation of NADH, enzymatically generated by oxidation of glucose by GDH active site. Kinetic measurements of immobilized GDH activity was performed by UV-Vis measurement, giving access to the real amount of grafted enzymes for each [**RuQ-pyrene**]/[**NHS-pyrene**] concentration ratio. As expected from the larger association constant K_{Ru} compared to K_{NHS} and fromthe bigger size of the enzyme compared to the polypyridine Ru^{II} complex, a similar amount of enzymes were immobilized on MWCNT whatever the ratio of the two pyrene derivatives,. The latter, 7.1 x 10^{-10} mol cm^{-2} of immobilized GDH, is approximatively equivalent to 8 compact enzyme layers, illustrating the efficient chemical grafting of GDH within the whole 3D structure of the MWCNT coating.[22] Moreover, this enzyme loading leads to a **RuQ-pyrene**/enzyme ratio of almost 260, assuming thus an efficient NADH oxidation.

The performances of bi-functionalized MWCNT electrodes were investigated by chronoamperometric measurements at 0.1V (figure 4C).Electrocatalytic currents increase with the increasing glucose concentration, according to a typical Michaelis-Menten dependence, reaching high catalytic currents of 1.95 mA cm^{-2} at 5mM glucose and maximum catalytic currents of 6.0 mA cm^{-2} at 70mM glucose. A calibration curve for glucose biosensing was obtained with a sensitivity of 0.27 mA mM^{-1} cm^{-2} with a detection limit of 10 µM (inset, figure 4C). This is among the best performances for glucose oxidation based on NAD-dependant GDH. High-performance previously-reported GDH-based bioanodes exhibited maximum currents of 0.4 mA cm^{-2} for hydrogel/CNT composite[23], 1.5 mA cm^{-2} for microfluidic-based bioelectrodes[24] or 4.1 mA cm^{-2} for NADH and poly-L-lysine-entrapped GDH on carbon fibers[1].

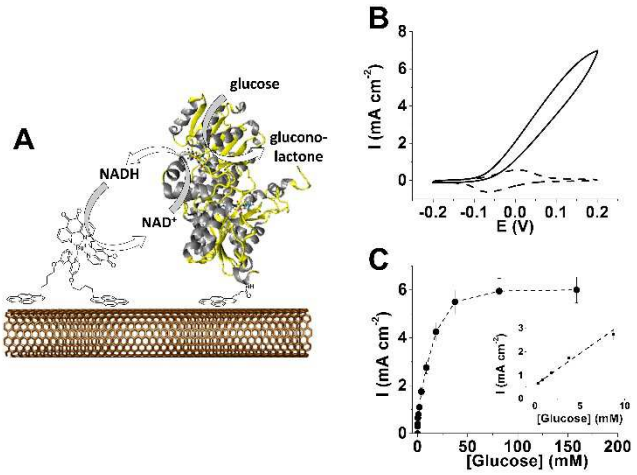

Figure 4. (A) Schematic representation of the preparation of the bi-functionalized MWCNT electrode with **RuQ-pyrene** catalystand GDH. (B) Cyclic voltammograms of RuQ-pyrene/GDH-functionalized MWCNT electrode in absence (dashed line) and presence (full line) of glucose (160 mM) in phosphate buffer (0.2M, pH 7) containing 10 mM NAD+ at 37°C (v= 10 mV s-1). (C) Calibration curve for glucose between 0 and 160 mM and in the linear range (inset). Applied potential 0.1V vs SCE in 0.2 M stirred phosphate buffer (pH7) containing 10mM NAD^+ at 37°C.

The soft and efficient supramolecular functionalization with an original pyrene-modified Ru^{II} complex and GDH affords the easy double functionalization of MWCNT electrodes, while ensuring maximum surface coverage of both molecular catalysts and biocatalysts. Furthermore, fine control over functionalization was assessed by a competitive Langmuir isotherm model, underlining the different interactions of modified pyrene molecules. Thanks to low overpotentials and high current densities, these functionalized MWCNT films show great promise for the design of novel bioelectrodes, especially for biofuel cell applications.

Acknowledgements

The Région Rhones-Alpes is acknowledged for the PhD funding of B. Reuillard. The authors also thank the ANR-12-JS08-0006-01 PHOBIOS for financial support. The authors wish to acknowledge the support from the platform Chimie NanoBio ICMG FR 2607 (PCN-ICMG) and from the LabEx ARCANE (ANR-11-LABX-0003-01).

Notes and references

[a] Univ. Grenoble Alpes, DCM UMR 5250, F-38000 Grenoble, France
CNRS, DCM UMR 5250, F-38000 Grenoble, France.
alan.le-goff@ujf-grenoble.fr
serge.cosnier@ujf-grenoble.fr

Electronic Supplementary Information (ESI) available: [Experimental details and figure S1]. See DOI: 10.1039/b000000x/

1. H. Sakai, T. Nakagawa, Y. Tokita, T. Hatazawa, T. Ikeda, S. Tsujimura, and K. Kano, *Energy Environ. Sci.*, 2008, **2**, 133–138.

ChemComm Accepted Manuscript

2. Y. H. Kim, E. Campbell, J. Yu, S. D. Minteer, and S. Banta, *Angew. Chem. Int. Ed.*, 2013, **52**, 1437–1440.
3. W. Jia, G. Valdés-Ramírez, A. J. Bandodkar, J. R. Windmiller, and J. Wang, *Angew. Chem. Int. Ed.*, 2013, **52**, 7233–7236.
4. S. Kochius, A. O. Magnusson, F. Hollmann, J. Schrader, and D. Holtmann, *Applied Microbiology and Biotechnology*, 2012, 2251–2264.
5. A. A. Karyakin, Y. N. Ivanova, K. V. Revunova, and E. E. Karyakina, *Anal. Chem.*, 2004, **76**, 2004–2009.
6. A. A. Karyakin, E. E. Karyakina, W. Schuhmann, and H. L. Schmidt, *Electroanalysis*, 1999, **11**, 553–557.
7. C. A. Goss and H. D. Abruna, *Inorg. Chem.*, 1985, **24**, 4263–4267.
8. B. Reuillard, A. Le Goff, and S. Cosnier, *Anal. Chem.*, 2014.
9. A. Le Goff, M. Holzinger, and S. Cosnier, *Analyst*, 2011, **136**, 1279–1287.
10. A. Le Goff, V. Artero, B. Jousselme, P. D. Tran, N. Guillet, R. Metaye, A. Fihri, S. Palacin, and M. Fontecave, *Science*, 2009, **326**, 1384–1387.
11. J. D. Blakemore, A. Gupta, J. J. Warren, B. S. Brunschwig, and H. B. Gray, *J. Am. Chem. Soc.*, 2013, **135**, 18288–18291.
12. P. Kang, S. Zhang, T. J. Meyer, and M. Brookhart, *Angew. Chem. Int. Ed.*, 2014, DOI: 10.1002/anie.201310722.
13. P. D. Tran, A. Le Goff, J. Heidkamp, B. Jousselme, N. Guillet, S. Palacin, H. Dau, M. Fontecave, and V. Artero, *Angew. Chem. Int. Ed.*, 2011, 1371–1374.
14. A. Le Goff, K. Gorgy, M. Holzinger, R. Haddad, M. Zimmerman, and S. Cosnier, *Chem. Eur. J.*, 2011, 10216–10221.
15. B. Reuillard, A. Le Goff, M. Holzinger, and S. Cosnier, *J. Mater. Chem. B*, 2014, **2**, 2228–2232.
16. S. Krishnan and F. A. Armstrong, *Chemical Science*, 2012, **3**, 1015–1023.
17. M. Bourourou, K. Elouarzaki, N. Lalaoui, C. Agnès, A. Le Goff, M. Holzinger, A. Maaref, and S. Cosnier, *Chem. Eur. J.*, 2013, 9371–9375.
18. C. Ménard-Moyon, C. Fabbro, M. Prato, and A. Bianco, *Chem. Eur. J.*, 2011, **17**, 3222–3227.
19. P. Singh, C. Ménard-Moyon, A. Battigelli, F. M. Toma, J. Raya, J. Kumar, N. Nidamanuri, S. Verma, and A. Bianco, *Chem. Asian J.*, 2013, **8**, 1472–1481.
20. M. Holzinger, J. Baur, R. Haddad, X. Wang, and S. Cosnier, *Chem. Commun.*, 2011, 2450–2452.
21. A. Le Goff and S. Cosnier, *J. Mater. Chem.*, 2011, **21**, 3910–3915.
22. C. Mousty, J.-L. Bergamasco, R. Wessel, H. Perrot, and S. Cosnier,*Anal.Chem.*,2001, 2890–2897.
23. M. T. Meredith, F. Giroud, and S. D. Minteer, *Electrochimica Acta*, 2012, **72**, 207–214.
24. M. Togo, A. Takamura, T. Asai, H. Kaji, and M. Nishizawa, *Electrochimica Acta*, 2007, **52**, 4669–4674.

ChemComm Accepted Manuscript

This journal is © The Royal Society of Chemistry 2012